Acta Cryst. (1975). A31, 435

Real-Space Methods for Interpreting Electron Micrographs in Cross-Grating Orientations. I. Exact Wave-Mechanical Formulation

BY A. M. OZORIO DE ALMEIDA*

Instituto de Física, Universidade Estadual de Campinas, 13100 *Campinas, São Paulo, Brazil*

(*Received* 6 *December* 1974; *accepted* 29 *January* 1975)

Alternative procedures are presented to the usual dynamical matrix method of calculating the dispersion surface, which suffers from very slow convergence in orientations where the diffraction pattern exhibits a full plane of the reciprocal lattice. A preliminary discussion is given of the cylindrical 'muffin-tin' approximation to the real-space projected crystal potential, the basis of the adaptation for use in high-energy electron-diffraction theory of both the APW and KKR methods. Full formulae for the diffracted amplitudes are arrived at, and an evaluation is made of the respective merits of the KKR and APW methods.

1. Introduction

Up to the present the computational ease of dealing with diffraction contrast images of crystals, oriented so as to give rise to a single row of diffraction spots, has ensured the popularity of 'systematic diffraction' work, as opposed to that using 'cross-grating' orientations, where a whole plane of diffraction spots is excited (see *e.g.* Berry, Buxton & Ozorio de Almeida, 1973, hereafter referred to as BBOA). It can be shown, within the conditions of validity of the high-energy approximation, that in the latter case the image is determined by a two-dimensional projection of the crystal potential, whereas in the former the effective potential has only one dimension (see *e.g.* Berry, 1971). This implies that the cross-grating image is by far the richer source of information on the full crystal potential, even if it is comparatively more difficult to extract. It also happens that for several materials it is much easier to prepare specimens to display cross-grating poles, *e.g.* epitaxically grown films and easily separable layered structures. For these reasons it is to be expected that interest in pole figures and methods for their interpretation is bound to grow, and first signs of this can already be found in the literature (Steeds, Jones, Ozorio de Almeida & Tatlock, 1973; Fujimoto *et al.*, 1973).

The standard many-beam 'dynamical' theory is in principle the simplest way to tackle the problem of electron motion in a two-dimensional lattice, or net of atomic strings, but, as in this instance the number of beams necessary for convergence is very great (typically of the order of 100), one must abdicate the physical insight provided by the analysis of approximations involving only a few beams even if adequate computational facilities are to be found. The advantage of working in real space is that one is able to make explicit use of the near cylindrical symmetry of the atomic strings so as to greatly reduce the labour of determining the dispersion surface. The full calculation of the diffraction amplitudes is still a formidable problem as we shall see, but use of the approximations discussed in part II (Ozorio de Almeida, 1975) when valid will greatly simplify this task. There, it will also be shown how some qualitative features of pole patterns can be sorted out using the present approach prior to any computation.

Part I contains a full wave-mechanical formulation of the KKR and APW methods of constructing the dispersion surface. The only approximation involved is the use of 'muffin-tin' potentials described in §3. Though the view of the author is that the strength of these methods will ultimately depend on the reliability of the approximations presented in part II and on their serving as a basis for the study of special effects of pole figures yet to be explored, there is no reason why they cannot be used as they stand. It should be mentioned that there are still other ways of calculating the diffracted amplitudes which altogether bypass the need to construct the dispersion surface. One is the *'multi-slice method'* [recently reviewed by Goodman & Moodie (1974)], which as the name implies, divides the crystal into layers thin enough to be considered separately as pure phase objects. This will certainly be the best method for very thin crystals. A full exposition of its application in cross-grating situations is to be found in Turner (1967). The method of *interfering classical paths*, considered in the first four sections of BBOA cannot be used reliably in the energy range of the common transmission electron microscope ($\sim$100 kV).

2. Bloch waves in two dimensions

Identifying the z axis with the crystal direction nearly parallel to the incident beam of electrons, and placing the origin on the entrance surface as shown in Fig. 1, with the positive z direction into the crystal, we define $\mathbf{R}$ as a two-dimensional position vector $\perp Oz$, so that

* Previously in the H. H. Wills Laboratory of Physics, Bristol, England.

$\mathbf{r}=(x,y,z)=(\mathbf{R},z)$. The wave equation in the high-energy approximation is then

$$\{\nabla^2+k_0^2-\bar{U}(\mathbf{R})\}\psi(\mathbf{r})=0\,, \qquad (2.1)$$

where the *wave number* k_0 and the *reduced projected potential* $\bar{U}(\mathbf{R})$ are given by the relativistic expressions

$$k_0=\frac{1}{\hbar}(2m_0E+E^2/c^2)^{1/2} \qquad (2.2)$$

and

$$\bar{U}(\mathbf{R})=\frac{2}{\hbar^2}(m_0+E/c^2)\frac{1}{\Delta}\int_0^{\Delta}\mathrm{d}z\, V(\mathbf{R},z)\,, \qquad (2.3)$$

E being the kinetic energy and m_0 the rest mass of the electron, whereas $V(\mathbf{r})$ is the real lattice potential with periodicity Δ in the z direction. Separation of variables in (2.1) leads to

$$\psi(\mathbf{R},z)=\sum_j c_j\tau_j(\mathbf{R})\exp\{i(k_0^2-S_j)^{1/2}z\}\,, \qquad (2.4)$$

where $\tau_j(\mathbf{R})$ satisfies

$$\{\nabla_R^2+S_j-\bar{U}(\mathbf{R})\}\tau_j(\mathbf{R})=0\,, \qquad (2.5)$$

S_j being the 'two-dimensional energy'. The absence of back scattering implies that the boundary condition on the incoming surface is simply

$$\sum_j c_j\tau_j(\mathbf{R})=\exp\{i(\mathbf{K}_0\,.\,\mathbf{R})\}\,, \qquad (2.6)$$

$\mathbf{K}_0$ being the component of the wave vector $\perp z$.

From the two-dimensional periodicity of $\bar{U}(\mathbf{R})$ it follows that the solutions $\tau_j(\mathbf{R})$ will be *Bloch waves*, satisfying

$$\tau_j(\mathbf{R}+\mathbf{R}_i)=\exp\{i(\mathbf{K}_0\,.\,\mathbf{R}_i)\}\tau_j(\mathbf{R})\,, \qquad (2.7)$$

if $\mathbf{R}_i$ is a *net vector*, with the *Bloch vector* $\mathbf{K}_0$ identical with the component of the incident wave vector defined previously. The quantized eigenvalues S_j depend on $\mathbf{K}_0$, and if $S_j(\mathbf{K}_0)$ is plotted vertically above the horizontal plane defined by (K_{0x},K_{0y}) the result is the dispersion surface (for the relation between this definition of the dispersion surface and the one more commonly used see Appendix A).

The Fourier coefficients of the Bloch wave are given by

$$\beta_{\mathbf{G}}^j=\frac{1}{\alpha}\int_{\text{mesh}}\mathrm{d}^2R\,\tau_j(\mathbf{R})\exp(-i\mathbf{K}_{\mathbf{G}}\,.\,\mathbf{R})\,, \qquad (2.8)$$

the integration being carried over a unit Wigner–Seitz cell, or mesh as it is called in two dimensions, of area α, and where use is made of the definition

$$\mathbf{K}_{\mathbf{G}}=\mathbf{K}_0+\mathbf{G}\,, \qquad (2.9)$$

$\mathbf{G}$ being a vector of the *reciprocal net*. Since, from equation (2.6)

$$C_j^*=\alpha\beta_0^j \qquad (2.10)$$

the expression for the $\mathbf{G}$th *diffraction amplitude* $A_{\mathbf{G}}(\mathbf{K}_0,z)$, defined by

$$\psi(\mathbf{r})\equiv\sum_{\mathbf{G}}\exp\{i(\mathbf{k}_0+\mathbf{G})\,.\,\mathbf{r}\}A_{\mathbf{G}}(\mathbf{K}_0,z)\,, \qquad (2.11)$$

is seen to be

$$A_{\mathbf{G}}(\mathbf{K}_0,z)=\alpha\sum_j\beta_0^{j*}\beta_{\mathbf{G}}^j\exp(-iS_jz/2k_0)\,. \qquad (2.12)$$

In the present notation the *dynamical matrix* equation becomes

$$\sum_{\mathbf{G}'}\beta_{\mathbf{G}'}^j\{[S_j(\mathbf{K}_0)-(\mathbf{K}_0+\mathbf{G})^2]\delta_{\mathbf{G}\mathbf{G}'}-\bar{U}_{\mathbf{G}-\mathbf{G}'}\}=0\,. \qquad (2.13)$$

It is the difficulty of representing the crystal potential $\bar{U}(\mathbf{R})$ in a Fourier sum with few Fourier coefficients $\bar{U}_{\mathbf{G}}$, which makes it hard to use the dynamical theory. This is a pity since (2·13) provides directly the coefficients $\beta_{\mathbf{G}}^j(\mathbf{K}_0)$ necessary for a full calculation of the diffraction amplitudes.

3. Nature of the projected potential

Before proceeding to the derivation of alternative eigenvalue equations to (2.13) it is worth while considering more closely the two-dimensional projected potential, especially as this is not done in BBOA. To the extent that the crystal can be pictured as a superposition of spherical atomic potentials, it is evident

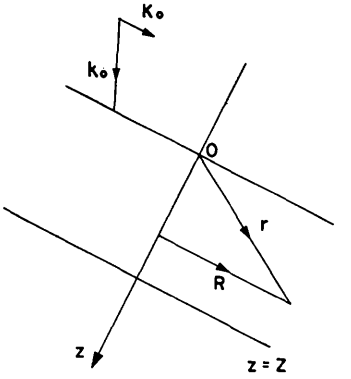

Fig. 1. Coordinate system.

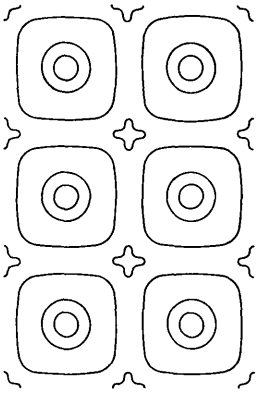

Fig. 2. Contours of constant $\bar{U}(\mathbf{R})$ for a square net.

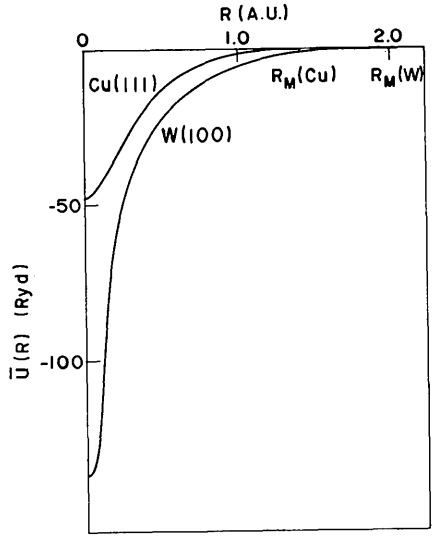

Fig. 3. Averaged potentials $\bar{U}(\mathbf{R})$ for an accelerating voltage of 750 kV.

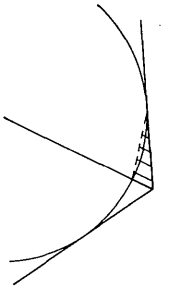

Fig. 4. Interstitial potential is obtained by first approximating the corner of the Wigner–Seitz mesh by linear potential in the triangle.

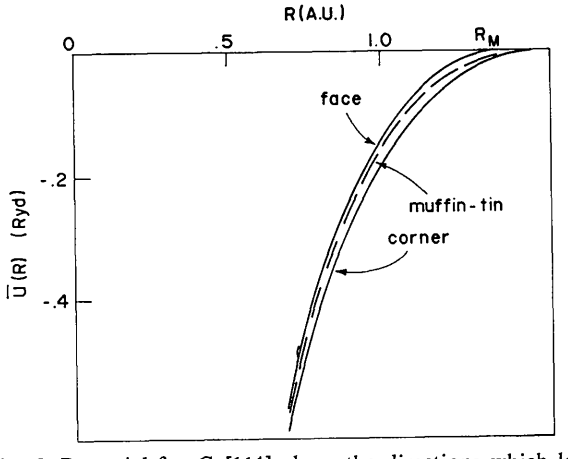

Fig. 5. Potential for Cu[111] along the directions which lead to the mesh corner and to the face centre is compared to the 'muffin-tin' potential near the 'muffin-tin' zero. The scale should be compared with that in Fig. 3.

that a single string of atoms would have a cylindrical averaged potential. The departure from pure radial dependence of the potential inside each Wigner–Seitz mesh will thus depend only on the small overlap of the different strings near the mesh boundaries and will be further reduced by any rotational symmetry of the lattice. Near the corners of the mesh the superposition of the string potentials will result in a flattening of the total (Fig. 2).

It is then reasonable to substitute the projected crystal potential by a cylindrical '*muffin-tin*' *model potential*: Inside the maximum circle that can be drawn about the centre of each string without overlapping neighbouring circles, the potential is made cylindrically symmetric, whereas outside these circles referred to as '*muffin-tins*', the interstitial potential is flat. The potential is then measured with respect to the interstitial potential; the '*muffin-tin*' *zero*. The great advantage of this model is that it enables angular momentum to be conserved in each Wigner–Seitz mesh.

Given the atomic scattering factors $f(s)$, found tabulated by say Doyle & Turner (1968), the projected real-space potential can be reconstructed from the Fourier series

$$\bar{U}(\mathbf{R}) = (-4\pi/\tau)\,(m/m_0) \times \sum_{\mathbf{G}} \exp(-\sigma^2 G^2/6) f(G/4\pi) \exp(i\mathbf{G}\cdot\mathbf{R}), \quad (3.1)$$

where τ is the volume of the primitive unit cell of the lattice, and $\sigma^2/6$ is the temperature-dependent Debye–Waller parameter. In the absence of lattice vibrations the projected potential would have a logarithmic singularity at the centre of the atomic strings, but this is smoothed over by the Debye–Waller factor (Fig. 3).

It can be verified that the angular average of $\bar{U}(\mathbf{R})$ required inside the muffin-tin is given by

$$\bar{U}(\mathbf{R}) = \text{const.} - (4\pi/\tau)\,(m/m_0) \sum_{\mathbf{G}} \exp(-\sigma^2 G^2/6) \times f(G/4\pi) J_0(GR), \quad (3.2)$$

$J_0(x)$ being a zero-order Bessel function. The arbitrary constant is determined from the fact that the average interstitial potential must be taken as the 'muffin-tin zero'. The most convenient way to estimate its value is to approximate the region by triangles, as shown in Fig. 4, and take the average of their corners. A comparison of the 'muffin-tin' potential for Cu[111] with that along the mesh diagonal and the bisector of the side of the mesh is shown in Fig. 5.

4. The KKR and APW eigenvalue equations

Experience with three-dimensional band-structure calculations shows that there are two outstanding methods making use of the near spherical 'muffin-tin' symmetry of the potential inside each Wigner–Seitz cell (see Ziman, 1971): the *Augmented Plane Wave* method, (Slater, 1973) know as the APW method, and the Greenian method known as the *KKR* method (Kor-

ringa, 1947; Kohn & Rostoker, 1954). The Greenian method is fully analytical, making it possible to obtain special insight into limiting regions of the dispersion surface. In three dimensions it is also the most convergent procedure. Unfortunately, however, it is not a viable way of obtaining exact diffraction amplitudes, since the wave functions are given in real-space angular-momentum representation throughout the Wigner–Seitz mesh. The APW method provides only an asymptotic approximation to the eigenvalues and Bloch functions. In spite of this the numerical convergence in three dimensions is almost as good as with KKR (see Lawrence, 1969). Moreover, in this method the wave functions are expanded in plane waves in the interstitial region of the unit mesh, which will be shown to facilitate the calculation of the Fourier integrals (2.8).

The presentation chosen to unify the derivation of the KKR and APW eigenvalue equations is closely modeled on that of Beleznay & Lawrence (1968), dealing with band structure in three dimensions. The reader may find that the original derivations of Slater, who followed a variational approach, and Korringa, based on multiple-scattering theory, are in many ways more instructive.

To solve equation (2.5) the lattice propagator or *Greenian* introduced, satisfying

$$(\nabla_{\mathbf{R}}^2+S)\,\mathscr{G}(\mathbf{R},\mathbf{R}')=\delta(\mathbf{R}-\mathbf{R}')\,. \tag{4.1}$$

Both wave function and propagator are subject to the Bloch condition on the boundary of a Wigner–Seitz cell:

$$\left.\begin{aligned} f(\mathbf{R}_0^b)&=\exp(i\mathbf{K}_0\,.\,\mathbf{R}_1)f(\mathbf{R}_1^b)\\ \frac{\partial}{\partial n}f(\mathbf{R}_0^b)&=-\exp(i\mathbf{K}_0\,.\,\mathbf{R}_1)f(R_1^b)\end{aligned}\right\} \tag{4.2}$$

where n is the unit outward pointing normal to the Wigner–Seitz cell boundary as shown in Fig. 6, and $\mathbf{R}_0^b$ and $\mathbf{R}_1^b$ are conjugate boundary points of the cell. Multiplying (2.5) by $\mathscr{G}^*(\mathbf{R},\mathbf{R}')$ and the complex conjugate of (4.1) by $\tau(\mathbf{R})$, subtracting the equations, and integrating over $\mathbf{R}$ in the interior of the polygonal mesh leads to

$$\int_{\text{W-S mesh}} \mathrm{d}^2R\,\mathscr{G}^*(\mathbf{R},\mathbf{R}')\bar{U}(\mathbf{R})\tau(\mathbf{R})-\tau(\mathbf{R})$$
$$=\oint_{\substack{\text{mesh}\\ \text{boundary}}}\left(\mathscr{G}^*\frac{\partial\tau}{\partial n}-\tau\frac{\partial\mathscr{G}^*}{\partial n}\right)\mathrm{d}s=0\,, \tag{4.3}$$

which, because of the Hermitian property

$$\mathscr{G}(\mathbf{R}',\mathbf{R})=\mathscr{G}^*(\mathbf{R},\mathbf{R}')\,, \tag{4.4}$$

is equivalent to

$$\tau(\mathbf{R})=\int_{\text{W-S mesh}}\mathrm{d}^2R'G(\mathbf{R},\mathbf{R}')\bar{U}(\mathbf{R}')\tau(\mathbf{R}')\,. \tag{4.5}$$

The lattice propagator can be expressed in terms of a real lattice sum

$$\mathscr{G}(\mathbf{R},\mathbf{R}')=(-i/4)\sum_{\mathbf{R}i}H_0^{(1)}(S^{1/2}|\mathbf{R}-\mathbf{R}'-\mathbf{R}_i|)\times\exp(i\mathbf{K}_0\,.\,\mathbf{R}_i)\,, \tag{4.6}$$

where $H_0^{(1)}(x)$ is a Hankel function, or expanded in terms of plane waves,

$$\mathscr{G}(\mathbf{R},\mathbf{R}')=1/\alpha\sum_{\mathbf{G}}\exp\{i\mathbf{K}_{\mathbf{G}}\,.\,(\mathbf{R}-\mathbf{R}')\}/(S-\mathbf{K}_{\mathbf{G}}^2)\,, \tag{4.7}$$

as can be directly verified by substitution into (4.1). The Hermitian property (4.4) is an obvious consequence of (4.7).

Transforming the volume integral over the 'muffin-tin' in (4.5) into a surface integral we obtain

$$\oint_{R'=R_M}\mathrm{d}s'\left\{\mathscr{G}(\mathbf{R},\mathbf{R}')\frac{\partial\tau(\mathbf{R}')}{\partial R'}-\tau(\mathbf{R}')\frac{\partial\mathscr{G}}{\partial R'}(\mathbf{R},\mathbf{R}')\right\}$$
$$+\int_{R'>R_M}\mathrm{d}^2R'\mathscr{G}(\mathbf{R},\mathbf{R}')\bar{U}(\mathbf{R}')\tau(\mathbf{R}')$$
$$=\begin{cases}\tau(\mathbf{R}) & (R>R_M) \qquad (4.8a)\\ 0 & (R<R_M)\,. \qquad (4.8b)\end{cases}$$

Thus, if $\bar{U}(\mathbf{R}')=0$ for $R>R_M$, where R_M is the 'muffin-tin' radius, the second term in the LHS of (4.8) is zero.

Substitution of the angular momentum expansion for the wave function,

$$\tau(\mathbf{R})=\tau(R,\theta)=\sum_{l=-\infty}^{\infty}a_l(R)\exp(il\theta) \tag{4.9}$$

and for the propagator,

$$\mathscr{G}(\mathbf{R},\mathbf{R}')=\tfrac{1}{4}\sum_{l,l'=-\infty}^{\infty}\{[-i\,J_l(S^{1/2}R)H_l^{(1)}(S^{1/2}R)\delta_{ll'}$$
$$+\mathscr{G}'_{ll'}(S,\mathbf{K}_0)J_l(S^{1/2}R)J_{l'}(S^{1/2}R)]$$
$$\times\exp(il\theta_{\mathbf{R}})\exp(il'\theta_{\mathbf{R}'})\}\,, \tag{4·10}$$

which defines the *structure constant* $\mathscr{G}'_{ll'}(S,\mathbf{K}_0)$, into equation (4.8*b*), and integration over angles leads to the set of homogeneous linear equations

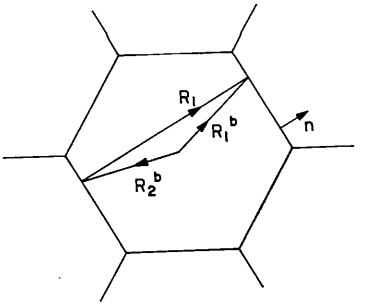

Fig. 6. Conjugate boundary points of the Wigner–Seitz mesh for a hexagonal net.

$$\sum_{l'=-\infty}^{\infty}\left\{\left[\frac{\partial}{\partial R'}H_{l'}^{(1)}(S^{1/2}R')-L_{l'}(S)H_{l'}^{(1)}(S^{1/2}R')\right]\delta_{ll'}+\mathscr{G}'_{ll'}(S,\mathbf{K}_0)\left[\frac{\partial}{\partial R'}J_{l'}(S^{1/2}R')-L_{l'}(S)J_{l'}(S^{1/2}R')\right]\right\}\times a_l(S,\mathbf{K}_0)=0 \tag{4.11}$$

where

$$L_l(S)=[1/\tau_l(R,S)]\left.\frac{d}{dR}\tau_l(R,S)\right|_{R=R_M}. \tag{4.12}$$

and $H_l^{(1)}(x)$ is a Hankel function. Finally, defining the two-dimensional analogue of the scattering *phase-shift* η_l,

$$\cot\eta_l(S)=\left\{\frac{\partial}{\partial R}\ Y_l(S^{1/2}R_M)-L_l(S)\,Y_l(S^{1/2}R_M)\right\}\div\left\{\frac{\partial}{\partial R}\ J_l(S^{1/2}R_M)-L_l(S)\,J_l(S^{1/2}R_M)\right\} \tag{4.13}$$

the eigenvalue condition becomes simply

$$\det\|(\cot\eta_l(S)-i)\delta_{ll'}+\mathscr{G}'_{ll'}(S,\mathbf{K}_0)\|=0\,. \tag{4.14}$$

The KKR method neatly separates all the structural aspects, into $\mathscr{G}'_{ll'}(S,\mathbf{K}_0)$, from the scattering properties of the individual 'muffin-tin' potential. In fact, the diagonal term is proportional to the inverse of the lth component of the scattering amplitude (see Berry & Ozorio de Almeida, 1973). The variational derivation of Kohn & Rostocker showed that any finite set of values a_l, obtained by truncating the infinite matrix equation (4.11) would give the best approximate fit to condition (4.8*b*) in some technical sense. A full discussion of the structure constants is left to Appendix B.

In the APW method the solution outside the 'muffin-tin' is expanded in a set of plane waves:

$$\tau(\mathbf{R})=\sum_{\mathbf{G}}B_{\mathbf{G}}(S,\mathbf{K}_0)\exp(i\mathbf{K}_{\mathbf{G}}\,.\,\mathbf{R})=\sum_{\mathbf{G}}B_{\mathbf{G}}\sum_l i^l J_l(K_{\mathbf{G}}R)\exp\{il(\theta_{\mathbf{R}}-\theta_{\mathbf{KG}})\}\,, \tag{4.15}$$

each plane wave being made continuous to a solution in the interior by the choice of the coefficients $C_l^{\mathbf{G}}$ in the expansion

$$\tau_{\mathbf{G}}(\mathbf{R})=\sum_{l=-\infty}^{\infty}C_l^{\mathbf{G}}\tau_l(R)\exp(il\theta_{\mathbf{R}})\,, \tag{4.16}$$

so that

$$C_l^{\mathbf{G}}=i^l J_l(K_{\mathbf{G}}R_M)\exp(-il\theta_{\mathbf{KG}})/\tau_l(R_M)\,. \tag{4.17}$$

By similarly expanding the Greenian:

$$\mathscr{G}(\mathbf{R},\mathbf{R}')=\frac{1}{\alpha}\sum_{\mathbf{G}}\{\exp(i\mathbf{K}_{\mathbf{G}}\,.\,\mathbf{R})/(S-K_{\mathbf{G}}^2)\}\times\sum_{l=-\infty}^{\infty}i^{-l}J_l(K_{\mathbf{G}}R')\exp\{-il(\theta_{\mathbf{R}'}-\theta_{\mathbf{KG}})\}\,, \tag{4.18}$$

equation (4.8) takes the form

$$\frac{2\pi R_M}{\alpha}\sum_{\mathbf{G},\mathbf{G}',l}[B_{\mathbf{G}'}\exp(i\mathbf{K}_{\mathbf{G}}\,.\,\mathbf{R})\exp\{il(\theta_{\mathbf{KG}}-\theta_{\mathbf{KG}'})\}\div(S-K_{\mathbf{G}'})]\times J_l(K_{\mathbf{G}}R)J_l(K_{\mathbf{G}'}R)\left\{L_l(S)-\times\frac{1}{J_l(K_{\mathbf{G}}R_M)}\frac{\partial}{\partial R}J_l(K_{\mathbf{G}}R_M)\right\}=\begin{cases}\psi(\mathbf{R}) & (R>R_M)\\ 0 & (R\le R_M)\end{cases}. \tag{4.19}$$

Defining $N_{\mathbf{GG}'}$ so that

$$\sum_{\mathbf{G}'}\exp(i\mathbf{G}'\,.\,\mathbf{R})N_{\mathbf{GG}'}=\begin{cases}\exp(i\mathbf{G}\,.\,\mathbf{R}) & (R\ge R_M)\\ 0 & (R\le R_M)\end{cases} \tag{4.20}$$

from which it follows that

$$N_{\mathbf{GG}'}=\frac{1}{\alpha}\int_{R>R_M}\exp\{i(\mathbf{G}-\mathbf{G}')\,.\,\mathbf{R}\}\,.\,\mathrm{d}^2R\,, \tag{4.21}$$

it is possible to combine the two regimes of equation (4.19) into the homogenous set of linear equations for the coefficients $B_{\mathbf{G}}$:

$$\sum_{\mathbf{G}'}\{(K_{\mathbf{G}}^2-S)N_{\mathbf{GG}'}+\Gamma^1_{\mathbf{GG}'}\}B_{\mathbf{G}'}=0\,, \tag{4.22}$$

with

$$\Gamma^1_{\mathbf{GG}'}=\frac{2\pi R_M}{\alpha}\sum_l J_l(K_{\mathbf{G}}R_M)J_l(K_{\mathbf{G}'}R_M)\times\exp\{il(\theta_{\mathbf{KG}}-\theta_{\mathbf{KG}'})\}\times\left\{L_l(S)-\frac{1}{J_l}\frac{\partial}{\partial R}J_l(K_{\mathbf{G}}R_M)\right\} \tag{4.23}$$

and

$$N_{\mathbf{GG}'}=N_{\mathbf{G}'\mathbf{G}}=\delta_{\mathbf{GG}'}-\frac{2\pi R_M}{\alpha}\frac{J_1(|\mathbf{G}-\mathbf{G}'|R_M)}{|\mathbf{G}-\mathbf{G}'|}\,. \tag{4.24}$$

It is possible to simplify formulae (4·22) and (4·23) in a way that shows each matrix element to be real: Making use of the derivative with respect to $K_{\mathbf{G}}$ of both sides of the identity

$$J_0(|\mathbf{K}_{\mathbf{G}}-\mathbf{K}_{\mathbf{G}'}|R_M)\equiv\sum_{l=-\infty}^{\infty}J_l(K_{\mathbf{G}}R_M)\times J_l(K_{\mathbf{G}'}R_M)\exp\{il(\theta_{\mathbf{KG}}-\theta_{\mathbf{KG}'})\}\,, \tag{4.25}$$

the APW eigenvalue formula becomes

$$\det\|(S-K_{\mathbf{G}}^2)\delta_{\mathbf{GG}'}-\Gamma_{\mathbf{GG}'}\|=0\,, \tag{4.26}$$

where the energy-dependent 'pseudopotential'

$$\Gamma_{\mathbf{GG}'}=\frac{2\pi R_M}{\alpha}\left\{-(\mathbf{K}_{\mathbf{G}}\,.\,\mathbf{K}_{\mathbf{G}'}-S)\frac{J_1(|\mathbf{G}-\mathbf{G}'|R_M)}{|\mathbf{G}-\mathbf{G}'|}\right. \tag{4.27}$$

$$\left.+\sum_{l=0}^{\infty}\varepsilon_l J_l(K_{\mathbf{G}}R_M)J_l(\mathbf{K}_{\mathbf{G}'}R_M)L_l(S)\times\cos l(\theta_{\mathbf{KG}}-\theta_{\mathbf{KG}'})\right\}\,,$$

and

$$\varepsilon_l=\begin{cases}1 & (l=0)\\ 2 & (l\ne 0)\end{cases}. \tag{4.28}$$

It is important to note that any departure from zero of the interstitial potential is easily taken into account by the APW method by simply adding a term

$$\bar{U}_{GG'} = \frac{1}{\alpha}\int_{R>R_M} d^2R\bar{U}(\mathbf{R}) \exp\{i(\mathbf{G}-\mathbf{G}') \cdot \mathbf{R}\} \tag{4.29}$$

to $\Gamma_{GG'}$.

5. Wave functions and Fourier coefficients

Once the eigenvalue $S_j(\mathbf{K}_0)$ has been found, the eigenvector a_l^j or B_G^j and hence the wave function $\psi(\mathbf{r})$ at the exit face of the crystal is determinable to within a constant factor. In general to do so is considerably more time-consuming than the evaluation of the determinant. The further problems of normalization and Fourier inversion are particular to the real-space methods described in the previous section. This is because the normalization condition implied by equation (2.10),

$$\int_{\text{mesh}} |\tau_j(\mathbf{R}_1\mathbf{K}_0)|^2 d^2R = 1 , \tag{5.1}$$

which in the dynamical theory reduces to the requirement that

$$\sum_{\mathbf{G}} |\beta_{\mathbf{G}}^j(\mathbf{K}_0)|^2 = 1/\alpha , \tag{5.2}$$

becomes in the KKR theory

$$\sum_{l,l'=-\infty}^{\infty} a_l^j a_{l'}^{j,*} \int_{\text{mesh}} d^2R\tau_l^j(\mathbf{R})\tau_{l'}^j(\mathbf{R}) \exp\{i(l-l')\theta_{\mathbf{R}}\} = 1 \tag{5.3}$$

and in the APW theory

$$\sum_{\mathbf{G},\mathbf{G}'} B_{\mathbf{G}}^j B_{\mathbf{G}'}^j \int_{\text{mesh}} d^2R\psi^j(\mathbf{R})\psi^{j*}(\mathbf{R}) = 1 , \tag{5.4}$$

where, of course

$$\psi^j(\mathbf{R}) = \begin{cases} \exp(i\mathbf{K}_{\mathbf{G}} \cdot \mathbf{R}) & (R > R_M) \\ C_l^{\mathbf{G}}\tau_l(R) \exp(il\theta_{\mathbf{R}}) & (R < R_M) \end{cases} . \tag{5.5}$$

There is no exact way of avoiding the two-dimensional integral over an area with non-separable boundaries required for the normalization of the KKR wave equation. The advantage of the APW method, in fact a hybrid between real and reciprocal space, is that the integral in (5.4) can be further simplified:

$$\begin{aligned} \int_{\text{mesh}} d^2R\psi^j(\mathbf{R})\psi^{j*}(\mathbf{R}) = \alpha N_{GG'} + 2\pi \sum_{l=0}^{\infty} \varepsilon_l \\ \times \cos l(\theta_{\mathbf{KG}} - \theta_{\mathbf{KG}'}) J_l(K_{\mathbf{G}}R_M) \\ \times J_l(K_{\mathbf{G}} \cdot R_M) \frac{1}{|\tau_l|^2} \\ \times \int_0^{R_M} RdR|\tau_l(R)|^2 \end{aligned} \tag{5.6}$$

and finally eliminated by making use of the relation (see *e.g.* Messiah, 1961)

$$\frac{1}{|\tau_l(R_M)|^2}\int_0^{R_M} RdR|\tau_l(R)|^2 = -R_M \frac{\partial L_l}{\partial S} . \tag{5.7}$$

Any computational procedure for finding the eigenvalues will involve the logarithmic derivative $L_l(S)$ at nearby points, which can easily be stored for the evaluation of (5.6) and (5.7). One can of course approximate the KKR Bloch functions by 'circularizing' the Wigner–Seitz mesh, *i.e.* by substituting in its place a circle with the same area. The integral in (5.3) then separates into a much simpler form than (5.6). Indeed for bound bands where $S_j < 0$, the partial waves $\tau_l(R)$ are exponentially small in the region of the cell which is fudged over, so that this approximation may be expected to hold very well.

After normalization one is in a position to evaluate the Fourier coefficients $\beta_{\mathbf{G}}^j$. The same problems again arise. The approximate circularized KKR Fourier coefficients are given by

$$\beta_{\mathbf{G}}^j \simeq \frac{2\pi}{\alpha} \sum_{l=-\infty}^{\infty} a_l^j \int_0^{R_{W-S}} RdR\tau_l^j(R)J_l(K_{\mathbf{G}}R) , \tag{5.8}$$

where R_{W-S} is the radius of the Wigner–Seitz circle. Fourier inversion of the APW wave function leads to

$$\begin{aligned} \beta_{\mathbf{G}}^j = \sum_{\mathbf{G}'} B_{\mathbf{G}}^j \Big\{ N_{GG'} + \frac{2\pi}{\alpha} \sum_{l=0}^{\infty} \varepsilon_l \cos l(\theta_{\mathbf{KG}'} - \theta_{\mathbf{KG}}) \\ \times \frac{J_l(\mathbf{K}_{\mathbf{G}'}R_M)}{\tau_l(R_M)} \int_0^{R_M} RdR\tau_l(R)J_l(K_{\mathbf{G}}R) \Big\} . \end{aligned} \tag{5.9}$$

6. Conclusion

The formulae of §4 are at present being tested against many-beam calculations of the dispersion surface. To proceed to a full simulation of pole figures one needs to take absorption into account. The way to do this is indicated in §6 of BBOA, the procedure being generalized to two dimensions in part II of this paper.

There is very little doubt that the 'muffin-tin' approximation, essential to the methods described, is excellent for the construction of the dispersion surface, and is also fairly reliable when dealing with average features of the wave-functions. Its value has yet to be tested, however, against anything like the fine features of cross-grating pole figures.

APPENDIX A

Relation between the usual definition of dispersion surface and the one adopted

Conventional dynamical theory considers the three-dimensional motion of the electrons under the influence of a lattice of aomtic strings or planes. This must have the form of a superposition of Bloch waves

$$\psi(\mathbf{r}) = \sum_j c_j \sum_{\mathbf{G}} \beta_{\mathbf{G}}^j \exp\{i(\mathbf{k}_j + \mathbf{G}) \cdot \mathbf{r}\} . \tag{A.1}$$

One then solves for $\psi(\mathbf{r})$ by inserting (A.1) directly into equation (2.1). The usual dispersion surface displays the $\mathbf{k}_j$ contours for constant k_0^2, but comparison of (A.1) with (2.12) and (2.11) shows that

$$\mathbf{k}_j = \mathbf{k}_0 - (S_j/2\,k_0)\hat{z}\,. \tag{A.2}$$

Thus, for a given $\mathbf{K}_0$, $(\mathbf{k}_j)_z$ and S_j are linearly related, it being necessary to turn upside down the solutions of equation (2.13) as well as to adjust the scale and the origin. Among other advantages it is much more convenient to draw S_j then to consider the small deviation k_j from $\mathbf{k}_0$. Finally it should be noted that in the Berry (1971) notation factors of 2π are included in the wave numbers and reciprocal-lattice vectors, which increases S_j and $\bar{U}(\mathbf{R})$ by a factor of $4\pi^2$.

APPENDIX B
The KKR structure constants

The *incomplete Greenian* $\mathscr{G}'(\mathbf{R},\mathbf{R}')$ is defined by

$$\mathscr{G}'(\mathbf{R},\mathbf{R}') = \mathscr{G}(\mathbf{R},\mathbf{R}') - \mathscr{G}^{\circ}(\mathbf{R},\mathbf{R}')\,, \tag{B.1}$$

where

$$\mathscr{G}^{\circ}(\mathbf{R},\mathbf{R}') = -\frac{i}{4} H_0^{(1)}(S^{1/2}|\mathbf{R}-\mathbf{R}'|) \tag{B.2}$$

is the *free propagator* in two dimensions. Both $\mathscr{G}(\mathbf{R},\mathbf{R}')$ and $\mathscr{G}^{\circ}(\mathbf{R},\mathbf{R}')$ satisfy equation (4.1), and so it follows that

$$(\nabla_{\mathbf{R}}^2 + S)\,\mathscr{G}'(\mathbf{R},\mathbf{R}') = 0 \tag{B.3}$$

in the unit mesh, which justifies the form taken by (4.10). The KKR structure constant is thus the angular-momentum representation of the incomplete Greenian.

To determine $\mathscr{G}'_{ll'}(\mathbf{K}_0,S)$ one expands the incomplete Greenian in terms of the single variable $\varrho \equiv \mathbf{R}-\mathbf{R}'$:

$$\mathscr{G}'(\varrho) = \sum_{l=-\infty}^{\infty} \mathscr{G}'_l(\mathbf{K}_0,S) J_l(S^{1/2}\varrho)\exp(il\theta_{\varrho})\,, \tag{B.4}$$

where there appears the *reduced structure constant*

$$\mathscr{G}'_l(\mathbf{K}_0,S) = -i\sum_{i\neq 0} H_l^{(1)}(S^{1/2}R_i) \times \exp\{i(\mathbf{K}_0\,.\,\mathbf{R}_i) - l\theta_{\mathbf{R}i})\}\,. \tag{B.5}$$

But, from methods similar to those found in Appendix 2 of Kohn & Rostoker (1954) we have that

$$J_l(S^{1/2}|\mathbf{R}-\mathbf{R}'|)\exp\{il(\theta_{\mathbf{R}}-\theta_{\mathbf{R}'})\} = \sum_{n,n'=-\infty}^{\infty} \delta_{l,n-n'} \times J_n(S^{1/2}R) J_{n'}(S^{1/2}R')\exp\{i(n\theta_{\mathbf{R}} - n'\theta_{\mathbf{R}'})\}\,, \tag{B.6}$$

thus arriving at the important result that the full structure constant

$$\mathscr{G}'_{ll'}(\mathbf{K}_0,S) = \mathscr{G}'_{l-l'}(\mathbf{K}_0,S) \tag{B.7}$$

and it is therefore only necessary to discuss the reduced structure constant. It should be noted that the relationship between $\mathscr{G}'_l$ and $\mathscr{G}'_{ll'}$ is much simpler in two than in three dimensions.

It is possible to obtain a reciprocal-lattice expansion of $\mathscr{G}'_l(\mathbf{K}_0,S)$ which is useful in theoretical considerations. Expansion in angular momentum of the plane wave in equation (4.7) and comparison with (B.4) gives

$$\mathscr{G}'_l(\mathbf{K}_0,S) = \frac{4il}{\alpha}\sum_{\mathbf{G}} \frac{\exp(-il\theta_{\mathbf{KG}})}{S-K_{\mathbf{G}}^2}\frac{J_l(K_{\mathbf{G}}\varrho)}{J_l(S^{1/2}\varrho)} + i\delta_{l,0}\frac{H_0^{(1)}(S^{1/2}\varrho)}{J_0(S^{1/2}\varrho)}\,. \tag{B.8}$$

For negative S the sum (B.5) for the reduced structure constant is rapidly convergent, but neither (B.5) nor (B.8) are efficient ways of evaluating $\mathscr{G}_l(\mathbf{K}_0,S)$ for positive energies. It is thus necessary to make use of a full Ewald scheme, first applied to the KKR equation by Ham & Segall (1961). This consists in splitting the summation into real-space and reciprocal-space series, both of which converge exponentially. Thus, writing

$$\mathscr{G}_l^1 = B_l^1 + B_l^2 + B_l^3\,, \tag{B.9}$$

we arrive at

$$\begin{aligned} B_l^1 &= \frac{4i^l}{\alpha} S^{-|l|/2}\sum_{\mathbf{G}} \frac{\exp\{(S-K_{\mathbf{G}}^2)X\}}{S-K_{\mathbf{G}}^2} K_{\mathbf{G}}^{|l|} \times \exp(-il\theta_{\mathbf{KG}}) \\ B_l^2 &= -\frac{2^{|l|}}{\pi} S^{|l|/2}\sum_{i\neq 0} R_i^{|l|} \times \exp\{i(\mathbf{K}_0\,.\,\mathbf{R}_i - l\theta_{\mathbf{R}_i})\} \times \int_{1/4X}^{\infty} \mathrm{d}t\, t^{|l|-1}\exp\{-R_i^2 t + S/4t\} \\ B_0^3 &= -\frac{1}{\pi}\delta_{l0}\int_{-\infty}^{Sx}\frac{\mathrm{d}u}{u}e^u = -\frac{1}{\pi}E_i(Sx)\,, \end{aligned} \tag{B.10}$$

where X can be chosen arbitrarily and $E_i(x)$ is the exponential integral function.

References

BELEZNAY, F. & LAWRENCE, M. J. (1968). *J. Phys. C: Solid State Phys.* **1**, 1288–1295.

BERRY, M. V. (1971). *J. Phys. C: Solid State Phys.* **4**, 697–721.

BERRY, M. V., BUXTON, B. F. & OZORIO DE ALMEIDA, A. M. (1973). *Rad. Eff.* **20**, 1–24.

BERRY, M. V. & OZORIO DE ALMEIDA, A. M. (1973). *J. Phys. A: Math. Gen.* **6**, 1451–1460.

DOYLE, P. A. & TURNER, P. S. (1968). *Acta Cryst.* **24**, 390–399.

FUJIMOTO, F., KOMAKI, K., FUJITA, H., SUMITA, N., UCHIDA, Y., KAMBE, K. & LEHMPFUHL, G. (1973). Private communication.

GOODMAN, P. & MOODIE, A. F. (1974). *Acta Cryst.* A**30**, 280–290.

HAM, F. S. & SEGALL, B. (1961). *Phys. Rev.* **124**, 1786–1796.

KOHN, W. & ROSTOKER, N. (1954). *Phys. Rev.* **94**, 1111–1120.
KORRINGA, J. (1947). *Physica*, **13**, 392–400.
LAWRENCE, M. J. (1969). Ph. D. Thesis, Univ. of Bristol.
MESSIAH, A. (1962). *Quantum Mechanics*. Vol. I. p. 100. Amsterdam: North Holland.
OZORIO DE ALMEIDA, A. M. (1975). *Acta Cryst.* A**31**, 442–445.
SLATER, J. C. (1937). *Phys. Rev.* **51**, 846–851.
STEEDS, J. W., JONES, P. M., OZORIO DE ALMEIDA, A. M. & TATLOCK, G. J. (1974). *High Voltage Electron Microscopy*, Edited by P. R. SWANN, C. J. HUMPHREYS & M. J. GORINGE. pp. 71–75. New York and London: Academic Press.
TURNER, P. S. (1967). Ph. D. Thesis, Univ. of Melbourne.
ZIMAN, J. M. (1971). *Solid State Phys.* **26**, 1.

Acta Cryst. (1975). A**31**, 442

Real-Space Methods for Interpreting Electron Micrographs in Cross-Grating Orientations. II. Analysis and Semiclassical Approximations

BY A. M. OZORIO DE ALMEIDA*

Instituto de Física, Universidade Estadual de Campinas, 13100 *Campinas, São Paulo, Brasil*

(*Received* 6 *December* 1974; *accepted* 29 *January* 1975)

The two-dimensional version of the KKR eigenvalue equation is analysed in different limiting situations. and reduction due to symmetry is discussed. With the aid of the semiclassical approximation to the Bloch functions, it is shown that simple expressions are obtained for the complex eigenvalues responsible for absorption. A qualitative understanding of some of the basic features of pole patterns results from a consideration of the approximations to both wave functions and dispersion surface.

1. Introduction

The main objective of the following discussion is to bring out the physical content of the formulae for the dispersion surface and the diffracted amplitudes contained in part I (Ozorio de Almeida, 1975). To begin with we analyse limiting regions of the two-dimensional dispersion surface, obtaining results which should remain approximately valid over wider domains, though this has yet to be computationally verified. Subsequently the results of §4 of Berry (1971) are generalized, leading to the semiclassical approximation of the Bloch functions. This in its turn permits one to deduce simple formulae for the imaginary components of the eigenvalues, which hold for all orientations. Finally, in §6, we begin to see how the preceding considerations can be directly applied to the understanding of pole patterns [see *e.g.* Berry, Buxton & Ozorio de Almeida (1973), again referred to as BBOA].

Symbols occurring in part I are not redefined here.

2. Approximations to the KKR eigenvalue equation

(i) *Born approximation*

In the weak scattering limit the assumption is made that the wave function in equation (4.5) of part I can be approximated by a plane wave:

$$\exp(i\mathbf{K}_0 \cdot \mathbf{R}) = \frac{1}{\alpha} \sum_{\mathbf{G}}{}^{-} \frac{\exp(i\mathbf{K}_\mathbf{G} \cdot \mathbf{R})}{S - K_\mathbf{G}^2} \times \int_{\text{mesh}} \mathrm{d}^2R' \bar{U}(R') \exp(-i\mathbf{G} \cdot \mathbf{R}') . \quad (2\text{–}1)$$

The Born approximation demands that all but the $\mathbf{G}=0$ term be neglected, leading to the eigenvalue condition

$$S^{\text{Born}} - K_0^2 = \langle \bar{U}(\mathbf{R}) \rangle . \quad (2.2)$$

This result, which also follows simply from perturbation theory (see Ziman, 1964), is not valid even for weak potentials at a zone boundary. A proof of condition (2.2) directly from the KKR eigenvalue equation is too involved to be included here, but it is worth pointing out that it involves summations to infinite order in angular momentum, thus indicating that use of the full KKR determinant to calculate the dispersion surface is not advisable when $S \gg \langle \bar{U}(\mathbf{R}) \rangle$.

The empty-lattice limit, $\langle \bar{U} \rangle \to 0$ in (2.2), is also satisfied by the APW equation, since a whole row ($\mathbf{G}=0$) of the determinant vanishes.

(ii) *Small-energy limit*

Analysis of the behaviour of phase shifts and structure constants shows that for $|S| \to 0$ the KKR determinant tends to a diagonal form. Except for anomalous cases referred to as *partial wave resonances*, when given phase shifts may tend to infinity, it is also

* Previously in the H. H. Wills Laboratory of Physics, Bristol, England.